International Journal of Hydrogen Energy 110 (2024) 787–796

Contents lists available at ScienceDirect

International Journal of Hydrogen Energy

journal homepage: www.elsevier.com/locate/he

Natural Hydrogen in the northern Semail Ophiolite: A case study in the Emirate of Ras Al Khaimah, UAE

Gabriel Pasquet [a,*], Keanu Loiseau [a], Mohamed Diatta [a], Giacomo Firpo [b], Paul Swire [b], Andrew Amey [b], Thibaut Burckhart [b], Isabelle Moretti [a]

[a] Laboratoire des Fluides complexes et de leurs Réservoirs (LFCR), UMR 5150, IPRA, Université de Pau et des Pays de l'Adour, Avenue de l'Université, 64000 Pau, France
[b] RAK Gas, Ras Al Khaimah, United Arab Emirates

ARTICLE INFO

Handling Editor: Dr. E.A. Veziroglu

Keywords:
Natural hydrogen
Semail Ophiolite
United Arab Emirates

ABSTRACT

The Semail Ophiolite provides a rare geological snapshot of oceanic lithosphere rocks at the surface. Extensive studies in the southern region, particularly within the Sultanate of Oman, have highlighted active serpentinization processes and the associated natural hydrogen (H_2) production. However, the northern region of the ophiolite remains underexplored. This study aims to fill this knowledge gap by investigating the potential natural H_2 resources in the Emirate of Ras Al Khaimah (RAK), in the United Arab Emirates (UAE). Comprehensive surface gas measurements allowed us to construct an H_2 distribution map which reveals H_2 presence and, as usual, show that the faults are preferential migration pathways. We also examine the correlation between gas emissions and lithological variations from the metamorphic sole to various mantle peridotites and crustal upper gabbros. Findings indicate that structural windows exposing the metamorphic sole are key areas for locating higher H_2 concentration measurements. Additionally, prominent structural lineaments between the layered and upper gabbros formations represent potential migration pathways for H_2 from the underlying peridotites. New alkaline *blue pools* (pH~9 and ongoing carbonation) have been identified; the gases sampled in these bubbling pools are very diversified. As in Oman, H_2-rich gas, up to 88% after air correction, have been found but also N_2 and CH_4-rich ones. A seasonal variation in the H_2/N_2 ratio was observed at one site, suggesting significant fluctuations within the underground water table, which is necessary for H_2 generation. These new measurements highlight the northern Semail Ophiolite's potential for natural H_2 exploration and production (E&P) in the RAK Emirate.

1. Introduction

The need for a more decarbonized energy mix has been widely recognized by many countries, and many stakeholders - governments, industries, research institutions and individuals - are actively working towards this goal. In this context, CO_2 capture and storage are seen as essential, as some industrial processes remain dependent on CO_2 emissions. The growing use of hydrogen (H_2) is another promising solution. H_2 is both an essential raw material in the chemical industry and a fuel capable of decarbonizing specific sectors, such as transport and industrial processes. However, the H_2 currently used in industry comes mainly from fossil fuels, such as methane and coal. The development of decarbonated H_2 alternatives is therefore a critical issue. While certain technologies, such as electrolysis, have reached a relatively advanced stage, their cost remains prohibitive compared to conventional methods of H_2 production, such as steam methane reforming. As a result, a number of alternative methods for producing decarbonized H_2 are being investigated. In many of these approaches, H_2 continues to be synthesized, for example by methane pyrolysis. However, there is a growing interest in exploring natural H_2 as a primary energy source, as it holds the potential to deliver a more environmentally sustainable energy supply [1,2].

1.1. Ras Al Khaimah legislation

The Ras Al Khaimah Petroleum Authority (RAKPA) has engaged various external parties with regards to regulating natural H_2, the conclusion from this work is that existing oil and gas Exploration and Production Sharing Agreements (EPSA's) are best modified for this purpose and this re purposing is currently being undertaken. Concurrently a series of engagements with the geoscience department of the UAE Ministry of Energy and Infrastructure (MOEI) has led to an

* Corresponding author.
E-mail address: gabriel.pasquet@univ-pau.fr (G. Pasquet).

https://doi.org/10.1016/j.ijhydene.2025.02.259
Received 17 December 2024; Received in revised form 10 February 2025; Accepted 15 February 2025
Available online 22 February 2025

agreement and a Memorandum of Understanding (MOU) has been signed to allow data and information sharing for H_2 and also for Carbon Capture including Mineralization.

An initial third-party evaluation highlighted that significant subsurface risks remain regarding natural H_2, necessitating further work to identify and mitigate these risks. RAKPA and RAK Gas, the national oil and gas company, have adopted a two-pronged approach. One of these, the top-down approach, is discussed in this paper. The other utilizing Play Based Exploration (PBE) methodology for a bottom up approach has also been undertaken. Surveys such as Magnetotelluric (MT) are also being acquired to aid in determining thickness variations in the ophiolite across the acreage and to help with prospectivity definition. Initially some shallow wells (to 600 m) are also being planned for profiling the ophiolite and also to acquire fresh unweathered samples. Licensing to interested parties and license monitoring is the natural progression into 2025 and beyond. One party is already commiting to exploration through signed agreement initially and other interested parties are also being sought. The RAK road map for decarbonation is shown in Fig. 1.

1.2. Natural H_2

Natural H_2 has been identified in numerous geological settings and through a wide range of fluid-rock interactions. These various natural H_2 generation contexts have been classified into four groups [3]: (H_2_GR1) oceanic lithospheres, notably including ophiolites and oceanic ridges [4–7]; (H_2_GR2) cratonic and Proterozoic provinces, including Banded Iron Formations (BIFs) [8–11]; (H_2_GR3) uranium-rich provinces [12, 13]; and (H_2_GR4) organic-rich sedimentary basins [14,15].

The H_2_GR1 group is centered on redox reactions between ferromagnesian rocks, such as peridotites, and water. The reduction of water through the oxidation of ferrous iron in olivine generates H_2 (e.g. equation (1.1) [16]). The optimal reaction temperature ranges between 250 °C and 300 °C [17,18]. At low temperatures (<100 °C), the Fe-rich brucite previously produced can be oxidised to form Fe(III)-serpentine (e.g. equation (1.2) [19]) and also minerals like magnetite and hydroandradite [20], enabling the production of H_2.

$$\underset{\text{olivine}}{Mg_{1.8}Fe_{0.2}SiO_4} + H_2O \rightarrow \underset{\text{Fe}^{2+}-\text{serpentine}}{(Mg,Fe)_3Si_2O_5(OH)_4} + \underset{\text{Fe}-\text{brucite}}{(Mg,Fe)(OH)_2} + \underset{\text{magnetite}}{Fe_3O_4} + H_2 \quad (1.1)$$

$$\underset{\text{Fe}-\text{brucite}}{2Fe(OH)_2} + 2SiO_2 + H_2O \rightarrow \underset{\text{Fe}^{3+}\text{-serpentine}}{Fe_2Si_2O_5(OH)_4} + H_2 \quad (1.2)$$

2. The Semail Ophiolite

2.1. Geological settings

The Semail Ophiolite is a region of primary interest for understanding serpentinization processes (H_2_GR1), due to the quality of its outcrops. Various studies, notably through the ICDP Oman Drilling Project [21], have demonstrated the presence of H_2 in bubbling springs and in the soil of the southernmost massifs around the Jabal Akhdar, including the massifs of Haylayn, Bahla, and Wadi Tayin [22–26]. Our study focusses specifically in the northern part of the Semail Ophiolite, in the Khawr Fakkan and Aswad massifs (Fig. 2).

The Semail Ophiolite is located in the southeast of the Arabian Peninsula, along the northeastern margin of the Sultanate of Oman and the United Arab Emirates, separated from Iran by the Gulf of Oman. This ophiolite nappe extends over 500 km in length and reaches up to 100 km in width in certain areas. It forms part of a mountain range associated with the Alpine orogenic belt [27].

This mountain range is divided into three tectono-stratigraphic units: autochthonous (and para-autochthonous) units, allochthonous units, and post-orogenic units [28]. The autochthonous units consist of a Neoproterozoic crystalline basement, a Proterozoic-Paleozoic sedimentary basement, and a carbonate sedimentary cover that developed from the Middle Permian to the end of the Cretaceous. The autochthonous massifs include the Jabal Akhdar and Saih Hatat (Fig. 2). The allochthonous units comprise the Hawasina sedimentary nappes and the Semail Ophiolite, which were thrusted onto the Arabian platform. The Hawasina complex includes the volcano-sedimentary Dibba and Hatta zones. Finally, the post-orogenic units consist of a Cenozoic sedimentary cover that unconformably overlies the older units.

During the Permian, an extensional regime led to continental rifting and the development of intercontinental basins, such as the Hawasina Basin, which represent the early stages of the Neo-Tethys Ocean. This rifting event is linked to the Pan-African orogeny. In the Lower Cretaceous, with the onset of the Alpine orogeny, the tectonic regime shifted to compression, resulting from convergent forces between the Eurasian and Arabian plates [29] this marked the initial phase of the Neo-Tethys Ocean's closure. Two significant volcanic episodes were recorded during the Cenomanian: V1 is related to the accretion of oceanic crust at a mid-ocean ridge while V2 is associated with the closure of the Neo-Tethys Ocean [30,31]. Several models were proposed to explain the formation of the Semail Ophiolite. One model suggests intra-oceanic thrusting [29], while others propose a fore-arc or rear-arc supra--subduction zone setting [32]. During the Turonian-Campanian period, oceanic detachment continued, culminating in the thrusting of oceanic sequences. Between 85 and 82 Ma, these oceanic units were accreted onto the passive continental margin of Oman [33]. The Maastrichtian marked the end of the obduction process, leading to the final emplacement of the Semail Ophiolite and subsequent isostatic rebalancing of the region. Following the obduction, the Omani continental margin experienced a series of transgression-regression cycles from the Maastrichtian to the Oligocene. Between the Oligocene and the early Miocene, during the Alpine orogenic phase, the Arabian plate continued its northeastward motion in relation to the Red Sea and Gulf of Aden opening [34–36]. These tectonic movements caused the uplift and subsequent erosion of the mountain ranges in Oman and the UAE, leading to the ophiolitic nappe being fragmented into 12 distinct massifs.

The Semail Ophiolite preserves the composition and structure of

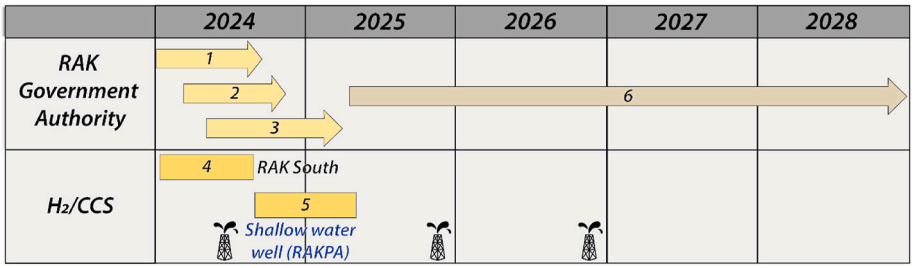

Fig. 1. RAK road map for decarbonation. CCS for Carbon Capture and Storage. The well icon corresponds to the planning of shallow wells for fresh sample acquisition. (1) Regulation drafting. (2) Liaison across government departments. (3) Implementation. (4) H_2 studies. (5) Magnetotelluric acquisitions. (6) Licensing and monitoring.

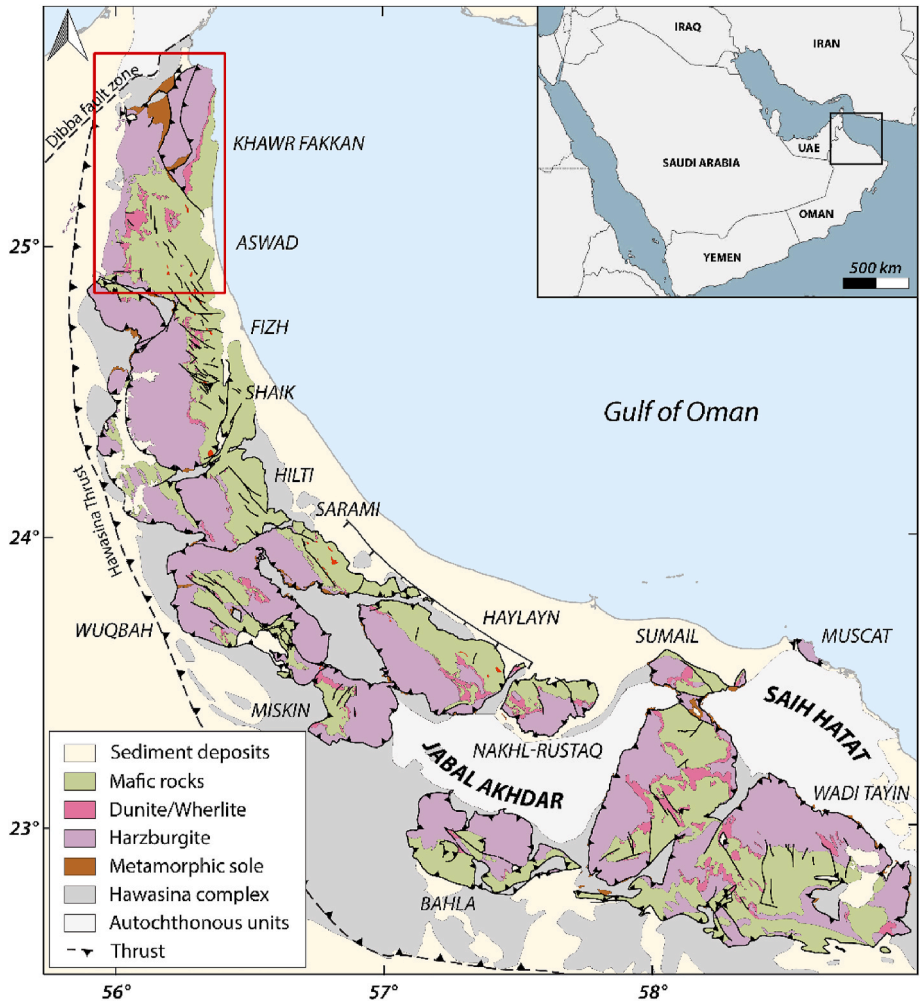

Fig. 2. Lithological units of the Semail Ophiolite, with the study area outlined in red (modified after Nicolas et al. [38]). (For interpretation of the references to colour in this figure legend, the reader is referred to the Web version of this article.)

Tethyan oceanic lithosphere, corresponding to a fast-spreading ridge environment [37,38]. It is primarily composed of pillow basalts, sheeted dikes, gabbros, and upper mantle peridotites, arranged in a stratigraphic sequence from top to bottom [29,39,40]. The upper mantle section, consisting of harzburgites and dunites, exhibits a thickness ranging from 12 to 15 km.

The lateral movement of the ophiolite over the underlying units has resulted in the formation of a metamorphic sole, which developed under pressure-temperature (P-T) conditions reaching 770–900°C and 11–15 kbar. This metamorphic basement, identified in the Bani Hamid and Masafi tectonic windows (UAE), is characterized by a vertical succession of granulite, amphibolite, and schist from top to bottom [41].

2.2. Hydrothermalism in the ophiolite

Throughout its evolution, the oceanic lithosphere experienced several episodes of alteration due to various fluid circulation processes. These included oceanic hydrothermal circulation, fluid movement during intra-oceanic detachment, and subsequent surface and meteoric fluid circulation after the emplacement of the ophiolite [42]. These fluid flows facilitated the serpentinization and carbonation of peridotites [17]. It is challenging to estimate the inherited rate of serpentinization during the initial stages of oceanic lithosphere formation at the ridge and off-axis, as well as that acquired during obduction and current onshore hydrothermal processes. However, after a petrographic study in which the different vein generations are distinguished, oxygen isotope analyses on serpentine or calcite can provide formation temperature data [43]. These data may be correlated with the various geodynamic stages [44]. Current serpentinization levels, in the Wadi Tayin massif, are estimated to average approximately 62% in harzburgites and 81% in dunites [39]. However, average serpentinization rates may not accurately reflect local variability and may differ substantially at all scale across a massif and, consequently, across other massifs as well [45].

Ongoing low-temperature (23°C–60 °C [20]) water-rock reactions, such as serpentinization and carbonation, of peridotites are evidenced in the Oman Drilling Project (DP) wells [46] and at alkaline spring sites, called blue pools, through travertine precipitation and carbonate veins within mantellic rocks [17,47]. In these springs, free gas is observed, with compositions divided into three main types reaching up to 93.8 vol % H_2, 92.0 vol% N_2 and 50.5 vol% CH_4 [22,24,25]. Often associated with active serpentinization within the ophiolite, H_2 is also detected in the soil of sub-ophiolitic units in the Jabal Akhdar and Hawasina regions [26].

3. Materials and methods

In an ophiolitic context, the main process to generate H_2 is the oxidation of Fe-rich minerals associated to the reduction of water [48–50]. To confirm the presence of deep H_2 generation, or leakage from accumulations, abnormal H_2 content in the soil or spring were measured and sampled [3,51].

3.1. Soil gas analysis

For soil measurements, we used a field gas analyzer called BIOGAS 5000. Our version measures six gases: CH_4 (%), CO_2 (%), O_2 (%), H_2 (ppmv), CO (ppmv), and H_2S (ppmv), as well as the balance (%), which corresponds to non-analyzed gases and is typically interpreted as being close to the N_2 content. The analyzer measures CH_4 and CO_2 using a dual-wavelength infrared sensor, while O_2, CO, H_2, and H_2S are detected using internal electrochemical cells. The measurement uncertainty for the values mentioned in the results is ±0.5% for CH_4 and CO_2, ±1.0% for O_2, and ±2.5%, ±2.0%, and ±2.0% for H_2, CO, and H_2S, respectively. The depth of the measurement is classically between 20 and 80 cm (length of the drilling bit), when rocks aren't directly outcropping in these areas where few soils have been developed. Recent measurements have shown that H_2 values between 1 and 5 m are not constant but remain within the same order of magnitude [52]. This behavior is similar to that of CO_2, as observed by Klusman [53], despite an increase of few percent in concentration between 30 and 100 cm. Shallow measurements consistently yield a high air content and therefore a lower percentage of other gases. Sporadic emanations are measured, then a single value can't be considered as representative [3,54]. Accordingly, a minimum of three measurements was conducted at each location, with a spacing of a few tens of centimeters, but only the maximum values are plotted (Fig. 3 and Table A.1). The resulting mapping can therefore be interpreted in terms of structural patterns related to the H_2 migration pathways of a given area, rather than a purely quantitative indicator.

3.2. Bubbling spring analysis

We located four bubbling seeps in a water spring (Fig. 3), allowing us to obtain quantitative gas concentration measurements. By analogy with alkaline to hyperalkaline springs with H_2-rich seeps, as described in the Oman case study [22,23,26], we draw comparisons to our findings. The gas was sampled by collecting bubbles in a septum-sealed funnel and injected into 10 mL vials using a gas tight syringe. The gas-tight syringe prevents gas exchange with the atmosphere before injection. These 10 mL vials allow us to determine the gas composition by gas chromatography (GC), and coupled with this GC, a mass spectrometer (GC-MS) enables us to analyze the isotopic composition of the gases for hydrogen (H), carbon (C), and nitrogen (N). The H_2, O_2+Ar, N_2, CO_2, CH_4 and hydrocarbons are analyzed on an Agilent 6890 N/7890A/7890 B GC using three detectors. A TCD detector for H_2, O_2+Ar, N_2 and CH_4, another TCD detector for CO_2 and a FID detector for hydrocarbons. From the results of all three detectors, one complete composition is calculated. Detector responses are calibrated several times a day using various reference standards. At least three vials were collected per bubbling site: two for major gas compositions (including one duplicate) and one for isotopic compositions. For the major gas composition, standard deviations are below 2% for concentrations above 1 mol% and below 10% for concentrations below 1 mol%. For isotopic compositions, three

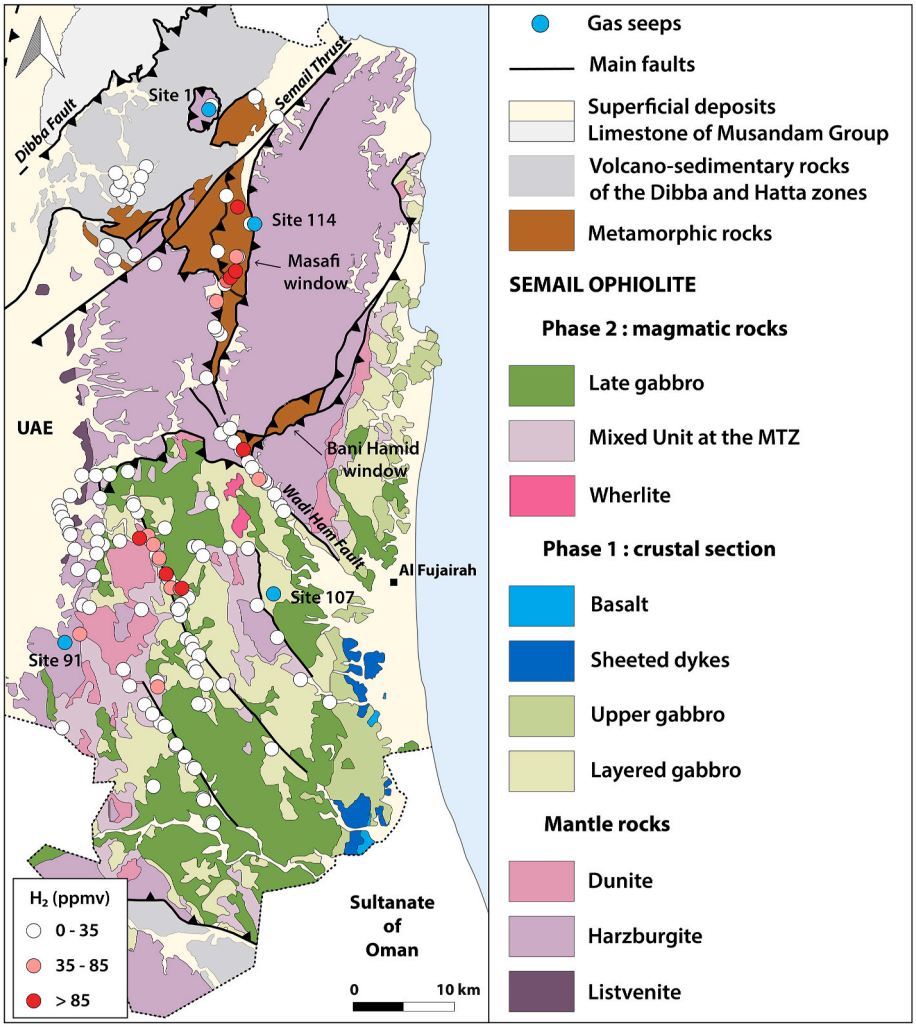

Fig. 3. H_2 soil measurements displayed on the geological map of the Semail Ophiolite centered on the UAE (see location Fig. 2), as well as gas sampling sites in blue (geological contours after [56]). (For interpretation of the references to colour in this figure legend, the reader is referred to the Web version of this article.)

measurements are performed on the same vials to assess measurement repeatability. The reported results represent the average of these three measurements, with standard deviations provided in Table 3. Furthermore, measurements of pH and water temperature were taken directly on site using a portable analyzer.

4. Results

4.1. Soil gas

In combining different missions, 488 gas measurements were carried out at 145 sites in the study area. Not surprisingly, Fig. 3 highlights the role of the faults in the fluid migration, and a trend emerges with the highest values on the large NW-SE lineaments in Ras Al Khaimah (RAK) South.

The highest values, in addition to being on major lineaments, are at the contact between the Layered Gabbro (GbL) and Mixed Unit (Mu) formations, with 121 ppmv, in RAK South. This transition between Mu and GbL is the crust-mantle transition.

To the north and northeast, the highest values are found in the sub-ophiolitic metamorphic windows. In the Masafi Shale Formation (MSF4), with 88 ppmv, for the Bani Hamid window; and in the Tayyibah Metavolcanic formation (TMv), with 171 ppmv, for the Masafi window.

Using a quantile-quantile graphical representation [55] of soil H_2 data (Fig. 4), two inflection points are observed, the first at 35 ppmv H_2 and the second at 85 ppmv H_2. From 0 to 35 ppmv, the values correspond to the soil gas atmosphere background in the area. From 35 to 85 ppmv, the values are more frequent and correspond to areas near potential H_2 emission sources close to the main faults, while values above 85 ppmv likely represent active H_2 emission zones above main faults, according to the geological map. It should be noted that outside main lineaments values are often below the 35 ppmv anomaly (Fig. 3). Values above the second anomaly identified at 85 ppmv (Fig. 4) are located along the main southern lineament between GbL and Mu, as well as in the tectonic windows of Bani Hamid and Masafi.

Fig. 3 also shows the 4 sites where free-gas were sampled. Site 1 corresponds to a bubbling blue-pools on a klippe of harzburgite north of the Semail Thrust. Site 91 corresponds to a wadi on the western front of the ophiolite, in the harzburgites of RAK South. Site 107, is located in a wadi on the GbL Fm. east of the ophiolite. Site 114, is located in a wadi above the harzburgites, near the Masafi metamorphic window.

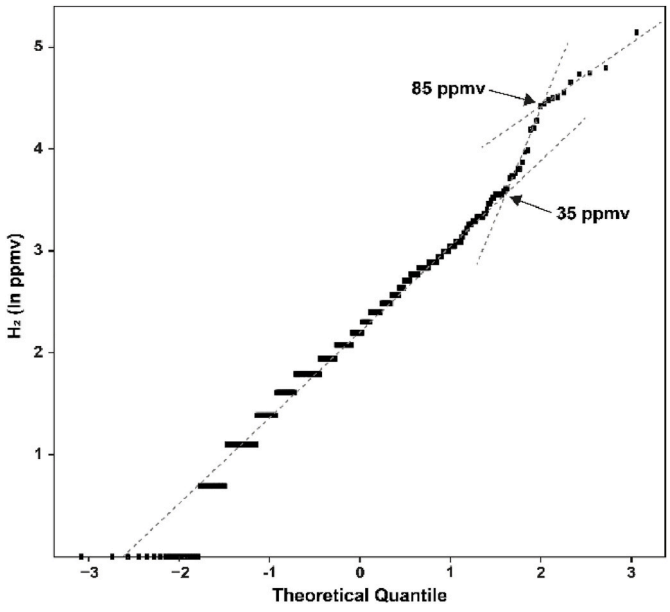

Fig. 4. Diagram showing the quantile-quantile plot calculated [55] for H_2 with two anomaly threshold values corresponding at 35 ppmv and 85 ppmv.

4.2. Bubbling springs

Gas composition and isotopes measurements were carried out on these 4 different sites (Figs. 3 and 5), representing 5 samples because two were taken at site 1. The results are listed in Tables 1–3 below. The gases, after air correction [57,58], appear to be blends. Results show that 3 major end-members stand out, the H_2-rich type with site 114, the CH_4-rich type with site 91 and the N_2-rich type with sites 1. It should be noted that site 107 shows an abnormally high oxygen concentration. Also, all sites are poor in CO_2.

Table 2 and Fig. 5 show temperatures (measured 5 cm below the water surface) ranging from 25.5 to 29.3 °C and pH levels between 8.09 and 9.31 in these blue pools and wadis where gas samples were collected. Fig. 5a illustrates the alkaline nature of Site 1 and 1', where substantial carbonate precipitation is observed, appearing as travertine or carbonate veins within the serpentinized massif. These carbonate precipitations were also observed in the wadi of Site 114, but were absent in the wadi Site 91 and 107.

The isotopic values in Table 3 show that the most H_2-rich sites with 44.6% and 87.8% (see Table 2), respectively on 1' and 114, have very homogeneous $\delta^{15}N$, $\delta^{13}C$ and δD isotopic values. The equilibrium temperatures associated with these sites on the CH_4–H_2 pair [59] are 66.6 °C and 44.9 °C for 1' and 114 respectively. Site 91, rich in CH_4, shows relatively similar isotopic values for $\delta^{13}C_{CO2}$ and δD_{CH4}, but a $\delta^{13}C_{CH4}$ reaching values of −61.5‰. Giving an equilibrium temperature in CO_2 and CH_4 [60] around 108 °C.

5. Discussion

5.1. Soil gas

As shown by the soil measurements in the field, the high H_2 values (>85 ppmv of H_2, Fig. 3) are associated with seepage along large faults bringing the GbL and Mu units into contact at surface and connecting at depth in the mantle peridotites. Soil measurements have also shown that the metamorphic basement, observed in the Masafi and Bani Hamid tectonic windows, on which the ophiolite has moved on, can play the role of H_2-generating rock. Values are higher in the metamorphic sole as observed in the Jabal Akhdar [26]. The fact that no H_2 is found in the non-fractured outcropping mantle and gabbro units (<35 ppmv), as also observed in southern massifs [26], may suggest that the gabbro units act as a cap for the H_2 system. Indeed, these gabbros are low in porosity and permeability compared to the mantle section below. The GbL from the CM1A well in the Wadi Tayin massif, drilled during the Oman DP campaigns, indicate a transport porosity of 0.12% and a calculated permeability from the core resistivity of 5.39×10^{-21} m^2 [61]. The dolerites sealing the H_2 reservoir at Bourakebougou have a total porosity of 0.39% [62]. However, the permeability of the gabbros may vary at the massif scale depending on fracture density. The large draining faults facilitate the migration of H_2 (Fig. 3) generated in the underlying volcanic, sediment-rich mantle or metamorphic basement. In the different context of stimulated H_2 by injecting water in ophiolites, the gabbro could be a lateral seal [63].

5.2. Bubbling springs and dry gas seepages

5.2.1. Gas origins

Site 114, rich in H_2, is totally consistent with gas measurements made in the southern part of the ophiolite in Oman and described in the literature as shown in Fig. 6. The N_2 pole of site 1 is generally observed in sediment-hosted formations in Jabal Akhdar (Fig. 6). Site 1', after air correction, is close to the N_2–H_2-rich group, commonly measured in the ophiolites of New Caledonia, Philippines and Oman [22,25]. CH_4-rich sites are uncommon in Semail and have more often been described in

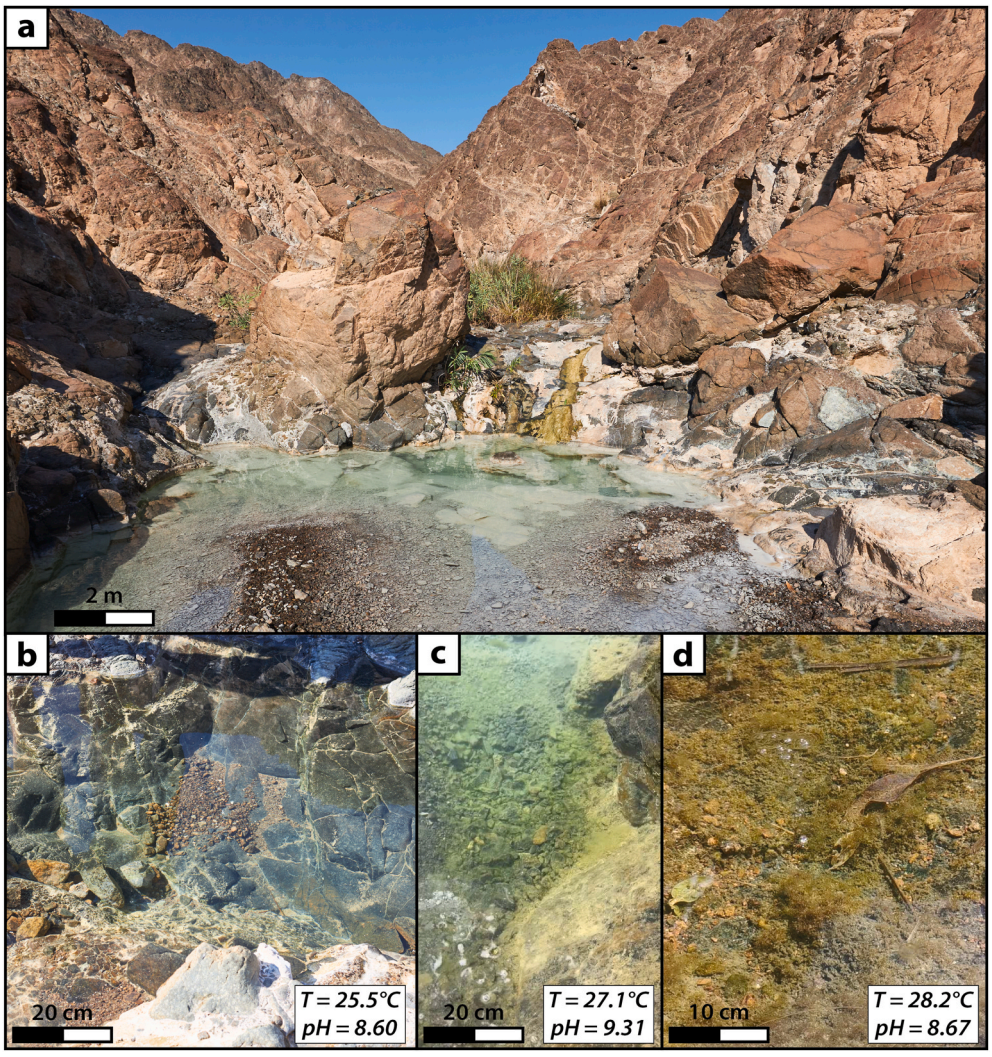

Fig. 5. Photographs of the various gas sampling sites. (a) Alkaline springs on the Harzburgite klippe downstream from (b) sites 1 and (c) 1'. (d) Carbonated spring rich in H_2 at site 114.

Table 1
Gas composition, in mol%, sampled at the various bubbling sites during the two surveys. Site 1 corresponds to bubbles taken during the first field acquisition, and site 1' from the same area during the second field acquisition. "bdl" stands for "below detection limit", corresponding to 0.04 mol% for H_2 and H_2S, 0.01 mol% for CO_2, O_2, and N_2, and 10^{-4} mmol% for hydrocarbons.

Sites	Latitude	Longitude	H_2	CH_4	N_2	O_2	CO_2	Ar	H_2S	C_2H_6	C_3H_8
			mol%	mol%	mol%	mol%	mol%	mol%	mol%	mmol%	mmol%
1	25.54399	56.155203	bdl	0.06	95.4	3.5	0.04	1.00	bdl	0.50	bdl
1'	25.5429384	56.15553363	16.50	0.22	69.20	13.20	0.01	0.84	bdl	0.50	1.00
91	25.07151935	56.01544456	bdl	78.30	16.20	2.40	2.60	0.46	bdl	0.60	0.20
107	25.114256	56.21195786	bdl	0.35	63.00	35.70	0.10	0.82	bdl	bdl	bdl
114	25.44023688	56.19892178	79.70	3.30	14.7	1.90	0.04	0.26	bdl	0.60	bdl

Table 2
Gas composition after air correction, in mol%, sampled at the various bubbling sites during the two surveys.

Sites	T	pH	H_2	CH_4	N_2	CO_2	Ar	C_2H_6	C_3H_8	$C_1/(C_2+C_3)$
	(°C)		mol%	mol%	mol%	mol%	mol%	mmol%	mmol%	
1	25.5	8.60	bdl	0.07	98.87	0.04	1.01	0.60	bdl	110
1'	27.1	9.31	44.64	0.59	54.08	0.00	0.68	1.35	1.00	253
91	26.3	8.09	bdl	88.47	8.20	2.93	0.40	0.68	0.20	100,761
107	29.3	8.73	bdl	0.00	98.91	0.00	1.09	Bdl	0.10	–
114	28.2	8.67	87.75	3.63	8.39	0.04	0.19	0.66	bdl	5500

Table 3
Isotopic compositions of gases at different sites, for $\delta^{15}N$, $\delta^{13}C$, δD and standard deviations in index of isotopic values, associated with gas equilibrium temperatures calculated for $T_{CO2\text{-}CH4}$ [60] and for $T_{CH4\text{-}H2}$ [59]

Sites	$\delta^{15}N$		$\delta^{13}C$				δD				$T_{CO2\text{-}CH4}$ (°C)	$T_{CH4\text{-}H2}$ (°C)
	‰ vs atm		‰ vs PDB				‰ vs SMOW					
	N_2		CH_4		CO_2		H_2		CH_4			
1’	+0.4	(0.0)	−5.9	(0.04)	−17.7	(0.06)	−729	(0.4)	−325	(1.2)		66.6
91	+2.5	(0.03)	−61.5	(0.17)	−15.9	(0.05)	–		−309	(1.0)	108.1	
107	0.0	(0.07)	−49.4	(0.02)	−19.5	(0.13)	–		−304	(0.2)	227.7	
114	+0.4	(0.08)	−10.6	(0.05)	−20.3	(0.09)	−733	(0.2)	−275	(0.3)		44.9

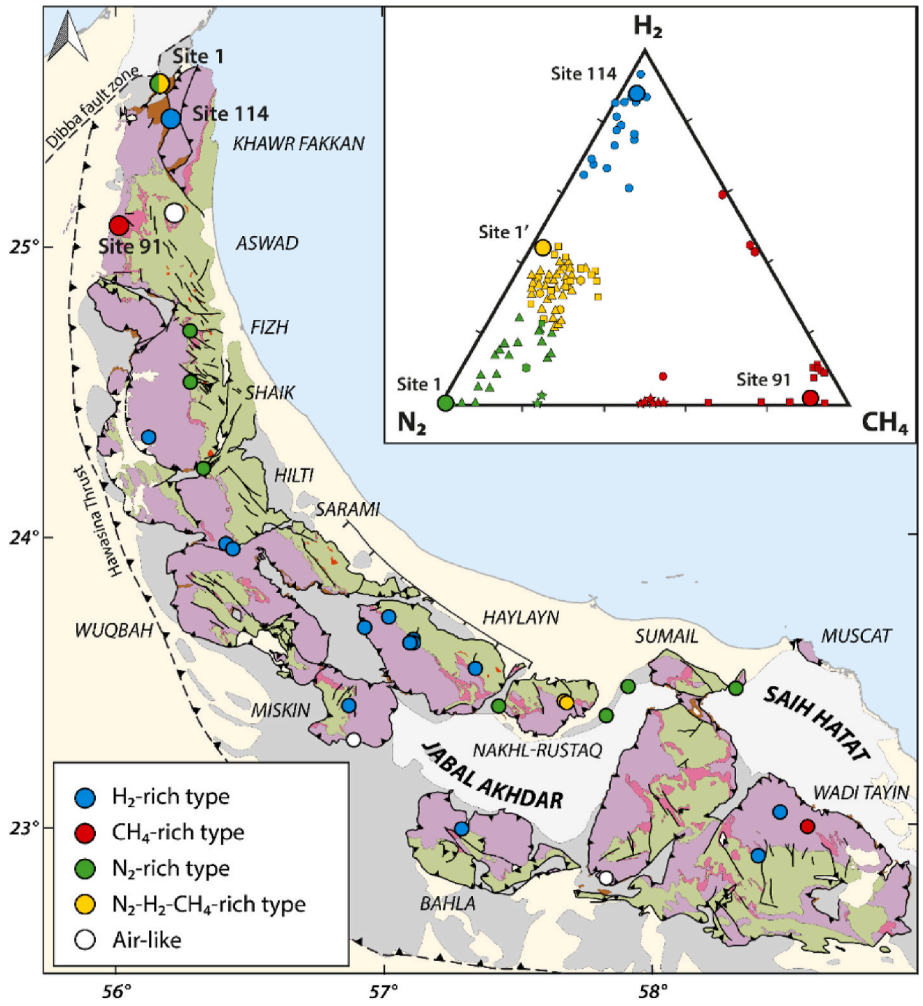

Fig. 6. Gas emanation map of the Semail Ophiolite, based on the geological map from Fig. 2 (modified after Nicolas et al. [38], showing the various bubbling springs measured and the types to which they belong. Ternary diagram illustrating the 3 end-members: H_2, N_2 and CH_4 of the different gas springs sampled, in the Semail Ophiolite (big circles are from this study in UAE and small circles from Oman), the Philippines ophiolites (hexagon), the Turkish ophiolites (square), the New Caledonian ophiolite (triangle) and the Italian ophiolites (star) [4,5,22–25,65,66].

Turkish ophiolites as gas seeping in fractures [25].

Fig. 7a shows a CH_4 origin associated with continental serpentinization for H_2-rich sites and a microbial CH_4 origin for site 91. Sites 1’ and 114 are perfectly correlated with measurements made south of the ophiolite in Oman, with low equilibrium temperatures (Table 3 and Fig. 7b). Fig. 7c supports the onshore origin of hydrogen in CH_4 and H_2, and Fig. 7d confirm this abiotic origin of CH_4 on sites 1’ and 114. Regarding $C_1/(C_2+C_3)$ ratio vs $\delta^{13}C_{CH4}$, this microbial origin is associated with a primary microbial reaction, close to methyl fermentation, for site 91 (Fig. 7d). O_2-rich sample, site 107, was taken in a water with high algae concentration, and therefore could reflect biosynthesis.

5.2.2. Seasonal variation of the gas content

Site 1, where we went twice, exhibits a temporal variation in gas composition, transitioning from an N_2-rich type to an N_2–H_2-rich mixture between November and April. This raises the question of the coexistence of two gas generation zones at the Masafi window, involving a constant crustal emission from the metamorphic sole and an intermittent serpentinization. Indeed, the two reactive zones [25,48] could be: a shallow zone fed by an aquifer with meteoric water circulating through the ultra-basic rocks forming these H_2-rich gases; a deeper zone coming from interstitial water, organic matter or ammonium trapped in the metamorphosed sediments of the sub-ophiolitic units. The N_2–H_2 mixture would then be a blend of these two sources. Thus, at site 1,

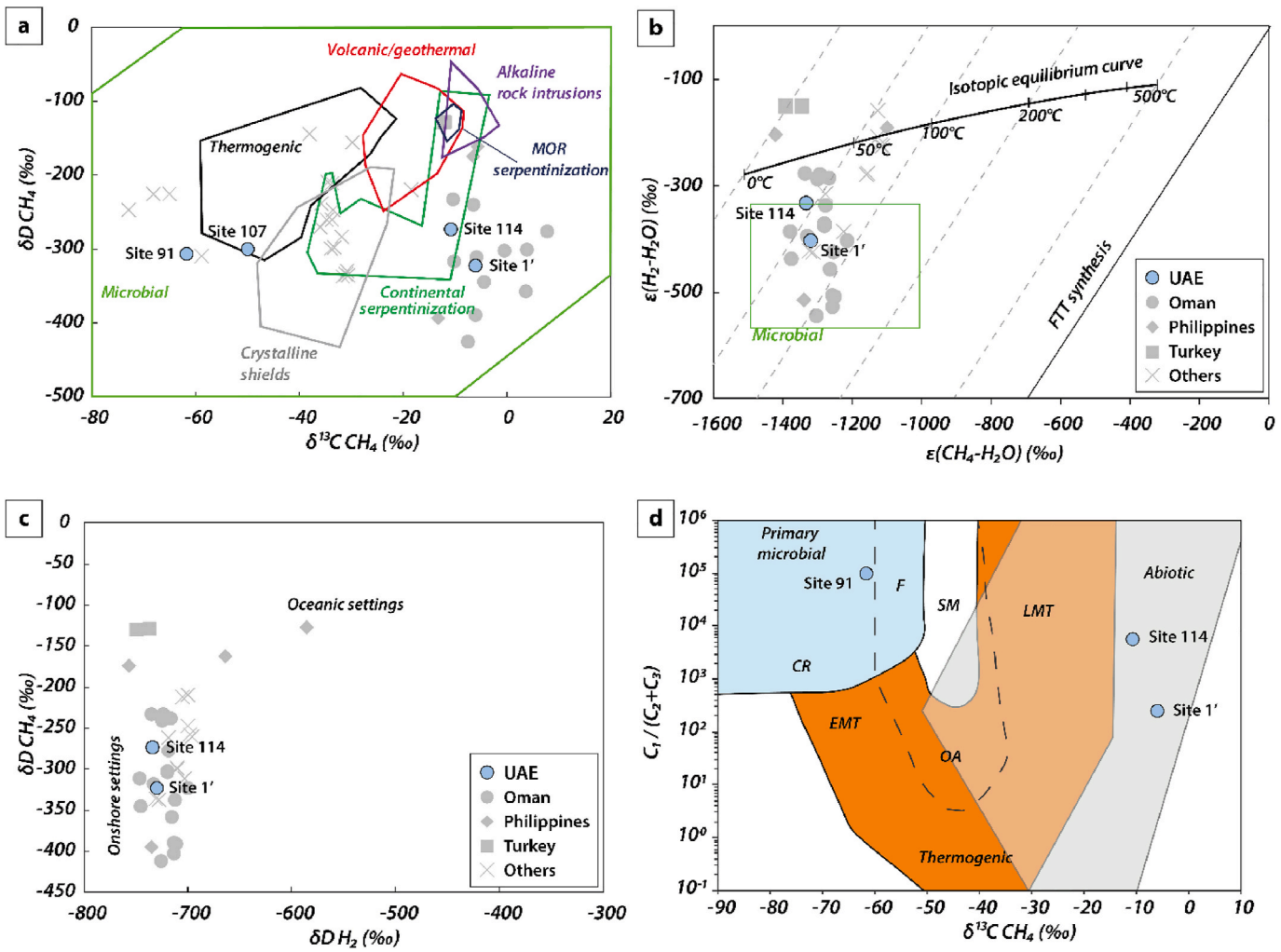

Fig. 7. Isotopic data from Semail Ophiolite sites, UAE. (a) δD CH_4 as a function of $\delta^{13}C$ CH_4, where different boxes are used to represent the origin of CH_4 (modified from Lévy et al. [3], Etiope [67], and Xia et al. [68]). (b) ε notation of H_2–H_2O and CH_4–H_2O pairs, representing whether the system is at thermodynamic equilibrium and determining the H_2–CH_4 equilibrium temperature (modified from Lévy et al. [3]). (c) δD CH_4 as a function of δD H_2 to compare the onshore or offshore nature of δD (modified from Vacquand et al. [25]). (d) Diagram of C1/(C2+C3) ratio as a function of $\delta^{13}C$ CH_4. With the genetic fields: CR=CO_2 reduction, F = methyl-type fermentation, SM = secondary microbial, EMT = early mature thermogenic gas, OA = oil-associated thermogenic gas, and LMT = late mature thermogenic gas (modified after Ketzer et al. [69]).

which varies between the N_2 and N_2–H_2-rich types, the hypothesis would be the presence of a non-permanent superficial aquifer that causes the gas ratios to vary when it is present or not. This hypothesis can be correlated with the regional climate, as the arid conditions here include a dry season extending from May to October, followed by a rainy season from November to March. Our samples from this site indicate 98.9% N_2 in November, just after the dry season, and 44.6% H_2 with only 54.1% N_2 in April, following the rainy season. We interpret this change as being due to the recharge of an aquifer or, at least, increased water saturation of the rocks.

Based on the temporal variability of gas concentrations and the isotopic $\delta^{13}C$ and δD data measured at H_2-rich sites 1' and 114 (Table 3 and Fig. 7), we can infer that the H_2 system is active, currently driven by onshore low-temperature serpentinization (between 45 and 66 °C), as suggested in Al Farfar (Bani Hamid window) [64].

At site 114, serpentinization of the peridotites is dominant, and this N_2-rich crustal source does not appear to be present or is highly diluted. This suggests the presence of a permanent shallow aquifer in the area.

$\delta^{15}N$ does not allow us to make final conclusions about the origin (atmospheric via an aquifer or crustal) of the N_2-rich gases in the ophiolites, analysis of noble gases will be more conclusive.

5.2.3. Regional variation of the gas content

Several factors may explain the variation in gas content observed throughout the Semail ophiolite (Fig. 6).

The primary lithological composition of peridotites can influence the measured hydrogen content. As shown by Stevens and McKinley [70], fayalite, followed by forsterite, will produce more H_2 during RedOx processes than pyroxene. Thus, for the same fluid, a serpentinized dunite will generate more H_2 than a harzburgite, which itself will produce varying amounts of H_2 depending on its pyroxene content (especially orthopyroxene). Similarly, fluid input into the system plays a major role in this production, as it enables the reduction processes responsible for H_2 formation. As demonstrated by Reed and Palandri [71], the nature of the fluid, whether fresh or saline, impacts both H_2 generation and transport. The accessibility of the fluid to these various Fe-bearing minerals is crucial. A higher connected porosity (and therefore higher permeability) increases the reactive surface area, potentially leading to greater H_2 production.

As shown by the seasonal variability discussed in the previous section, the timing of measurements across different massifs can influence these values, leading to results that fluctuate between H_2 and N_2 end-members.

Finally, CH_4 content is likely more dependent on the environmental

conditions in which these measurements are taken. A setting favorable to microbial activity could lead to higher CH_4 concentrations. Additionally, CH_4 may also form abiotically through the reaction of H_2 with CO or CO_2 via Fischer-Tropsch or Sabatier reactions. The CO and CO_2 involved in these processes can have multiple origins within the ophiolite, including mantle degassing, carbonate dissolution from the numerous pre-ophiolitic carbonate formations (e.g. Hawasina nappes), or oxidation of organic matter present in the pre-ophiolitic sediments.

6. Conclusion

These new gas data from the northern zone of the Semail Ophiolite demonstrate once again the suitability of this region for natural H_2 exploration. These data are very encouraging for potential future production, with gas emanation up to 87% of H_2 at surface in alkaline springs. In addition, soil and gas seeps data over time highlight the presence of a more or less continuous flow towards the surface along major faults in the ophiolite and tectonic windows (>85 ppmv of H_2). Soil gas measurements indicate a near surface background level <35 ppmv of H_2 within the ophiolite and the metamorphic sole. The upper crustal units (gabbros) may act as a seal for gas emissions.

The gas analyses are fully in line with what has been observed in the Sultanate of Oman, with the presence of the 3 major gas end-members (H_2-rich, N_2-rich and CH_4-rich) in the study area. The H_2-rich gases are interpreted as being associated with low-temperature continental serpentinization, with minima of 45 °C and 66 °C, based on isotopic values. The temporal variation in gas composition from N_2 to N_2–H_2 at Site 1, within the alkaline spring of the Harzburgite klippe, suggests continuous deep N_2 generation of crustal metamorphic origin and periodic shallow H_2 generation through serpentinization when groundwater circulation occurs. Water supply in this region appears to play a crucial role in the availability of H_2 resources. No source containing free gas has been observed in tectonic windows where the metamorphic sole is exposed to confirm soil measurements. The CH_4-rich source is interpreted as a dry gas seepage from a microbial origin.

The diversity of H_2-generating rocks, both mantellic and crustal metamorphic, only increases the field of possibilities for these sites of interest.

CRediT authorship contribution statement

Gabriel Pasquet: Writing – review & editing, Writing – original draft, Visualization, Methodology, Investigation, Formal analysis, Data curation, Conceptualization. **Keanu Loiseau:** Writing – review & editing, Investigation, Formal analysis. **Mohamed Diatta:** Writing – review & editing, Investigation, Formal analysis. **Giacomo Firpo:** Writing – review & editing, Validation, Supervision, Resources, Investigation. **Paul Swire:** Writing – review & editing, Validation, Resources, Investigation. **Andrew Amey:** Validation, Project administration, Funding acquisition. **Thibaut Burckhart:** Writing – review & editing, Validation, Project administration, Funding acquisition. **Isabelle Moretti:** Writing – review & editing, Validation, Supervision, Project administration, Investigation.

Funding

This work was supported by RAK Gas.

Declaration of competing interest

The authors declare that they have no known competing financial interests or personal relationships that could have appeared to influence the work reported in this paper.

Acknowledgements

The authors are grateful to RAK Gas for allowing us to collaborate, conduct fieldworks in the UAE and for funding this research. We also thank ISOLAB and B. Van Der Haven for the compositional and isotopic analyses of the gas samples.

Appendix A. Supplementary data

Supplementary data to this article can be found online at https://doi.org/10.1016/j.ijhydene.2025.02.259.

References

[1] Brandt AR. Greenhouse gas intensity of natural hydrogen produced from subsurface geologic accumulations. Joule 2023;7:1818–31. https://doi.org/10.1016/j.joule.2023.07.001.
[2] Gaucher EC, Moretti I, Pélissier N, Burridge G, Gonthier N. The place of natural hydrogen in the energy transition: a position paper. https://doi.org/10.5281/ZENODO.8108239; 2023.
[3] Lévy D, Roche V, Pasquet G, Combaudon V, Geymond U, Loiseau K, et al. Natural H 2 exploration: tools and workflows to characterize a play. Sci Tech Energy Transition 2023;78:27. https://doi.org/10.2516/stet/2023021.
[4] Abrajano TA, Sturchio NC, Bohlke JK, Lyon GL, Poreda RJ, Stevens CM. Methane-hydrogen gas seeps, Zambales Ophiolite, Philippines: deep or shallow origin? Chem Geol 1988;71:211–22. https://doi.org/10.1016/0009-2541(88)90116-7.
[5] Etiope G, Schoell M, Hosgörmez H. Abiotic methane flux from the Chimaera seep and Tekirova ophiolites (Turkey): understanding gas exhalation from low temperature serpentinization and implications for Mars. Earth Planet Sci Lett 2011;310:96–104. https://doi.org/10.1016/j.epsl.2011.08.001.
[6] Pasquet G, Idriss AM, Ronjon-Magand L, Ranchou-Peyruse M, Guignard M, Duttine M, et al. Natural hydrogen potential and basaltic alteration in the Asal–Ghoubbet rift, Republic of Djibouti. BSGF - Earth Sci Bull 2023;194:9. https://doi.org/10.1051/bsgf/2023004.
[7] Truche L, Donzé F-V, Goskolli E, Muceku B, Loisy C, Monnin C, et al. A deep reservoir for hydrogen drives intense degassing in the Bulqizë ophiolite. Science 2024;383:618–21. https://doi.org/10.1126/science.adk9099.
[8] Boreham CJ, Edwards DS, Czado K, Rollet N, Wang L, van der Wielen S, et al. Hydrogen in Australian natural gas: occurrences, sources and resources. APPEA J 2021;61:163. https://doi.org/10.1071/AJ20044.
[9] Moretti I, Geymond U, Pasquet G, Aimar L, Rabaute A. Natural hydrogen emanations in Namibia: field acquisition and vegetation indexes from multispectral satellite image analysis. Int J Hydrogen Energy 2022;47:35588–607. https://doi.org/10.1016/j.ijhydene.2022.08.135.
[10] Roche V, Geymond U, Boka-Mene M, Delcourt N, Portier E, Revillon S, et al. A new continental hydrogen play in Damara Belt (Namibia). Sci Rep 2024;14:11655. https://doi.org/10.1038/s41598-024-62538-6.
[11] Maiga O, Deville E, Laval J, Prinzhofer A, Diallo AB. Characterization of the spontaneously recharging natural hydrogen reservoirs of Bourakebougou in Mali. Sci Rep 2023;13:11876. https://doi.org/10.1038/s41598-023-38977-y.
[12] Leila M, Loiseau K, Moretti I. Controls on generation and accumulation of blended gases (CH4/H2/He) in the Neoproterozoic Amadeus Basin, Australia. Mar Petrol Geol 2022;140:105643. https://doi.org/10.1016/j.marpetgeo.2022.105643.
[13] Sherwood Lollar B, Onstott TC, Lacrampe-Couloume G, Ballentine CJ. The contribution of the Precambrian continental lithosphere to global H2 production. Nature 2014;516:379–82. https://doi.org/10.1038/nature14017.
[14] Horsfield B, Mahlstedt N, Weniger P, Misch D, Vranjes-Wessely S, Han S, et al. Molecular hydrogen from organic sources in the deep Songliao Basin, P.R. China. Int J Hydrogen Energy 2022;47:16750–74. https://doi.org/10.1016/j.ijhydene.2022.02.208.
[15] Mahlstedt N, Horsfield B, Weniger P, Misch D, Shi X, Noah M, et al. Molecular hydrogen from organic sources in geological systems. J Nat Gas Sci Eng 2022;105:104704. https://doi.org/10.1016/j.jngse.2022.104704.
[16] Templeton AS, Ellison ET. Formation and loss of metastable brucite: does Fe(II)-bearing brucite support microbial activity in serpentinizing ecosystems? Phil Trans R Soc A 2020;378:20180423. https://doi.org/10.1098/rsta.2018.0423.
[17] Kelemen PB, Matter J. In situ carbonation of peridotite for CO2 storage. Proc Natl Acad Sci USA 2008;105:17295–300. https://doi.org/10.1073/pnas.0805794105.
[18] Klein F. Compositional controls on hydrogen generation during serpentinization of ultramafic rocks. 2013.
[19] Klein F, Bach W, Jöns N, McCollom T, Moskowitz B, Berquó T. Iron partitioning and hydrogen generation during serpentinization of abyssal peridotites from 15°N on the Mid-Atlantic Ridge. Geochem Cosmochim Acta 2009;73:6868–93. https://doi.org/10.1016/j.gca.2009.08.021.
[20] Ellison ET, Templeton AS, Zeigler SD, Mayhew LE, Kelemen PB, Matter JM, et al. Low-temperature hydrogen formation during aqueous alteration of serpentinized peridotite in the samail ophiolite. J Geophys Res Solid Earth 2021;126:e2021JB021981. https://doi.org/10.1029/2021JB021981.
[21] Kelemen P, Al Rajhi A, Godard M, Ildefonse B, Köpke J, MacLeod C, et al. Scientific drilling and related research in the samail ophiolite, sultanate of Oman. Sci Dril 2013;15:64–71. https://doi.org/10.5194/sd-15-64-2013.

[22] Leong JA, Nielsen M, McQueen N, Karolytė R, Hillegonds DJ, Ballentine C, et al. H2 and CH4 outgassing rates in the Samail ophiolite, Oman: implications for low-temperature, continental serpentinization rates. Geochem Cosmochim Acta 2023; 347:1–15. https://doi.org/10.1016/j.gca.2023.02.008.
[23] Neal C, Stanger G. Hydrogen generation from mantle source rocks in Oman. Earth Planet Sci Lett 1983;66:315–20. https://doi.org/10.1016/0012-821X(83)90144-9.
[24] Sano Y, Urabe A, Wakita H, Wushiki H. Origin of hydrogen-nitrogen gas seeps, Oman. Appl Geochem 1993;8:1–8. https://doi.org/10.1016/0883-2927(93)90053-J.
[25] Vacquand C, Deville E, Beaumont V, Guyot F, Sissmann O, Pillot D, et al. Reduced gas seepages in ophiolitic complexes: evidences for multiple origins of the H2-CH4-N2 gas mixtures. Geochem Cosmochim Acta 2018;223:437–61. https://doi.org/10.1016/j.gca.2017.12.018.
[26] Zgonnik V, Beaumont V, Larin N, Pillot D, Deville E. Diffused flow of molecular hydrogen through the Western Hajar mountains, Northern Oman. Arab J Geosci 2019;12:71. https://doi.org/10.1007/s12517-019-4242-2.
[27] Hanna SS. The alpine deformation of the Central Oman mountains. SP, vol. 49; 1990. p. 341–59. https://doi.org/10.1144/GSL.SP.1992.049.01.21.
[28] Glennie KW. Geology of the Oman mountains. Royal Geological and Mining Society of the Netherlands (KNGMG); 1974.
[29] Coleman RG. Tectonic setting for ophiolite obduction in Oman. J Geophys Res 1981;86:2497–508. https://doi.org/10.1029/JB086iB04p02497.
[30] Rioux M, Bowring S, Kelemen P, Gordon S, Dudás F, Miller R. Rapid crustal accretion and magma assimilation in the Oman-U.A.E. ophiolite: high precision U-Pb zircon geochronology of the gabbroic crust: Oman ophiolite zircon geochronology. J Geophys Res 2012;117. https://doi.org/10.1029/2012JB009273. n/a-n/a.
[31] Rioux M, Garber J, Bauer A, Bowring S, Searle M, Kelemen P, et al. Synchronous formation of the metamorphic sole and igneous crust of the Semail ophiolite: new constraints on the tectonic evolution during ophiolite formation from high-precision U–Pb zircon geochronology. Earth Planet Sci Lett 2016;451:185–95. https://doi.org/10.1016/j.epsl.2016.06.051.
[32] Pearce JA, Alabaster T, Shelton AW, Searle MP. The Oman ophiolite as a Cretaceous arc-basin complex: evidence and implications. Phil Trans R Soc Lond A 1981;300:299–317. https://doi.org/10.1098/rsta.1981.0066.
[33] Rabu D, Nehlig P, Roger J. Stratigraphy and structure of the Oman mountains. Documents Du BRGM 1993;221:262.
[34] Bosworth W, Huchon P, McClay K. The Red Sea and Gulf of aden basins. J Afr Earth Sci 2005;43:334–78. https://doi.org/10.1016/j.jafrearsci.2005.07.020.
[35] Girdler RW. The evolution of the Gulf of aden and Red Sea in space and time. Deep-Sea Res Part A Oceanogr Res Pap 1984;31:747–62. https://doi.org/10.1016/0198-0149(84)90039-6.
[36] Stern RJ, Johnson P. Continental lithosphere of the Arabian Plate: a geologic, petrologic, and geophysical synthesis. Earth Sci Rev 2010;101:29–67. https://doi.org/10.1016/j.earscirev.2010.01.002.
[37] Goodenough KM, Styles MT, Schofield D, Thomas RJ, Crowley QC, Lilly RM, et al. Architecture of the Oman–UAE ophiolite: evidence for a multi-phase magmatic history. Arab J Geosci 2010;3:439–58. https://doi.org/10.1007/s12517-010-0177-3.
[38] Nicolas A, Boudier F, Ildefonse B, Ball E. Accretion of Oman and United Arab Emirates ophiolite – discussion of a new structural map. Mar Geophys Res 2000;21: 147–80. https://doi.org/10.1023/A:1026769727917.
[39] Boudier F, Coleman RG. Cross section through the peridotite in the samail ophiolite, southeastern Oman mountains. J Geophys Res 1981;86:2573–92. https://doi.org/10.1029/JB086iB04p02573.
[40] Glennie KW, Boeuf MGA, Clarke MWH, Moody-Stuart M, Pilaar WFH, Reinhardt BM. Late cretaceous nappes in Oman mountains and their geologic evolution. AAPG (Am Assoc Pet Geol) Bull 1973;57:5–27.
[41] Searle MP, Waters DJ, Garber JM, Rioux M, Cherry AG, Ambrose TK. Structure and metamorphism beneath the obducting Oman ophiolite: evidence from the Bani Hamid granulites, northern Oman mountains. Geosphere 2015;11:1812–36. https://doi.org/10.1130/GES01199.1.
[42] Dewandel B, Lachassagne P, Boudier F, Al-Hattali S, Ladouche B, Pinault J-L, et al. A conceptual hydrogeological model of ophiolite hard-rock aquifers in Oman based on a multiscale and a multidisciplinary approach. Hydrogeol J 2005;13:708–26. https://doi.org/10.1007/s10040-005-0449-2.
[43] Aupart C, Morales L, Godard M, Jamtveit B. Seismic faults triggered early stage serpentinization of peridotites from the Samail Ophiolite, Oman. Earth Planet Sci Lett 2021;574:117137. https://doi.org/10.1016/j.epsl.2021.117137.
[44] Lévy D, Callot J-P, Moretti I, Duttine M, Dubreuil B, De Parseval P, et al. Successive phases of serpentinization and carbonation recorded in the Sivas ophiolite (Turkey), from oceanic crust accretion to post-obduction alteration. BSGF - Earth Sci Bull 2022;193:12. https://doi.org/10.1051/bsgf/2022015.
[45] Loiseau K, Aubourg C, Petit V, Bordes S, Lefeuvre N, Thomas E, et al. Hydrogen generation and heterogeneity of the serpentinization process at all scales: Turon de Técouère lherzolite case study, Pyrenees (France). Geoenergy 2024;2. https://doi.org/10.1144/geoenergy2023-024. geoenergy2023-024.
[46] Kelemen PB, Leong JA, Carlos de Obeso J, Matter JM, Ellison ET, Templeton A, et al. Initial results from the Oman drilling Project multi-borehole observatory: petrogenesis and ongoing alteration of mantle peridotite in the weathering horizon. J Geophys Res Solid Earth 2021;126:e2021JB022729. https://doi.org/10.1029/2021JB022729.
[47] Noël J, Godard M, Oliot E, Martinez I, Williams M, Boudier F, et al. Evidence of polygenetic carbon trapping in the Oman Ophiolite: petro-structural, geochemical, and carbon and oxygen isotope study of the Wadi Dima harzburgite-hosted carbonates (Wadi Tayin massif, Sultanate of Oman). Lithos 2018;323:218–37. https://doi.org/10.1016/j.lithos.2018.08.020.
[48] Deville E, Prinzhofer A. The origin of N2-H2-CH4-rich natural gas seepages in ophiolitic context: a major and noble gases study of fluid seepages in New Caledonia. Chem Geol 2016;440:139–47. https://doi.org/10.1016/j.chemgeo.2016.06.011.
[49] Klein F, Tarnas JD, Bach W. Abiotic sources of molecular hydrogen on earth. Elements 2020;16:19–24. https://doi.org/10.2138/gselements.16.1.19.
[50] Truche L, McCollom TM, Martinez I. Hydrogen and abiotic hydrocarbons: molecules that change the world. Elements 2020;16:13–8. https://doi.org/10.2138/gselements.16.1.13.
[51] Pasquet G, Houssein Hassan R, Sissmann O, Varet J, Moretti I. An attempt to study natural H2 resources across an oceanic ridge penetrating a continent: the asal–ghoubbet rift (republic of Djibouti). Geosciences 2021;12:16. https://doi.org/10.3390/geosciences12010016.
[52] Patino C, Piedrahita D, Colorado E, Aristizabal K, Moretti I. Natural H2 transfer in soil: insights from soil gas measurements at varying depths. Geosciences 2024;14: 296. https://doi.org/10.3390/geosciences14110296.
[53] Klusman RW. Baseline studies of surface gas exchange and soil-gas composition in preparation for CO2 sequestration research: teapot Dome, Wyoming. Bulletin 2005;89:981–1003. https://doi.org/10.1306/03310504109.
[54] Moretti I, Prinzhofer A, Françolin J, Pacheco C, Rosanne M, Rupin F, et al. Long-term monitoring of natural hydrogen superficial emissions in a brazilian cratonic environment. Sporadic large pulses versus daily periodic emissions. Int J Hydrogen Energy 2021;46:3615–28. https://doi.org/10.1016/j.ijhydene.2020.11.026.
[55] Lefeuvre N, Truche L, Donzé F, Ducoux M, Barré G, Fakoury R, et al. Native H $_2$ exploration in the western pyrenean foothills. Geochem Geophys Geosyst 2021;22: e2021GC009917. https://doi.org/10.1029/2021GC009917.
[56] Ambrose TK, Searle MP. 3-D structure of the northern Oman-UAE ophiolite: widespread, short-lived, suprasubduction zone magmatism. Tectonics 2019;38: 233–52. https://doi.org/10.1029/2018TC005038.
[57] Bernard A, Battani A, Rizzo AL, Balci U, Györe D, D'Alessandro W, et al. Temporal monitoring of fumarole composition at Santorini volcano (Greece) highlights a quiescent state after the 2011–2012 unrest. Front Earth Sci 2024;12:1366213. https://doi.org/10.3389/feart.2024.1366213.
[58] Rizzo AL, Caracausi A, Chavagnac V, Nomikou P, Polymenakou PN, Mandalakis M, et al. Geochemistry of CO2-rich gases venting from submarine volcanism: the case of kolumbo (hellenic volcanic arc, Greece). Front Earth Sci 2019;7. https://doi.org/10.3389/feart.2019.00060.
[59] Horibe Y, Craig H. Fractionation in the system methane-hydrogen-water. Geochem Cosmochim Acta 1995;59:5209–17. https://doi.org/10.1016/0016-7037(95)00391-6.
[60] Bottinga Y. Calculated fractionation factors for carbon and hydrogen isotope exchange in the system calcite-carbon dioxide-graphite-methane-hydrogen-water vapor. Geochem Cosmochim Acta 1969;33:49–64. https://doi.org/10.1016/0016-7037(69)90092-1.
[61] Katayama I, Abe N, Hatakeyama K, Akamatsu Y, Okazaki K, Ulven OI, et al. Permeability profiles across the crust-mantle sections in the Oman drilling Project inferred from dry and wet resistivity data. J Geophys Res Solid Earth 2020;125: e2019JB018698. https://doi.org/10.1029/2019JB018698.
[62] Maiga O, Deville E, Laval J, Prinzhofer A, Diallo AB. Trapping processes of large volumes of natural hydrogen in the subsurface: the emblematic case of the Bourakebougou H2 field in Mali. Int J Hydrogen Energy 2023; S036031992305214X. https://doi.org/10.1016/j.ijhydene.2023.10.131.
[63] Templeton AS, Ellison ET, Kelemen PB, Leong J, Boyd ES, Colman DR, et al. Low-temperature hydrogen production and consumption in partially-hydrated peridotites in Oman: implications for stimulated geological hydrogen production. Front Geochem 2024;2:1366268. https://doi.org/10.3389/fgeoc.2024.1366268.
[64] Etiope G, Judas J, Whiticar MJ. Occurrence of abiotic methane in the eastern United Arab Emirates ophiolite aquifer. Arab J Geosci 2015;8:11345–8. https://doi.org/10.1007/s12517-015-1975-4.
[65] Boulart C, Chavagnac V, Monnin C, Delacour A, Ceuleneer G, Hoareau G. Differences in gas venting from ultramafic-hosted warm springs: the example of Oman and Voltri Ophiolites. Ofioliti 2013;38. https://doi.org/10.4454/ofioliti.v38i2.423.
[66] Monnin C, Quéméneur M, Price R, Jeanpert J, Maurizot P, Boulart C, et al. The chemistry of hyperalkaline springs in serpentinizing environments: 1. The composition of free gases in New Caledonia compared to other springs worldwide. J Geophys Res: Biogeosciences 2021;126:e2021JG006243. https://doi.org/10.1029/2021JG006243.
[67] Etiope G. Abiotic methane in continental serpentinization sites: an overview. Procedia Earth Planet Sci 2017;17:9–12. https://doi.org/10.1016/j.proeps.2016.12.006.
[68] Xia X, Gao Y. Validity of geochemical signatures of abiotic hydrocarbon gases on Earth. JGS 2022;179:jgs2021–j2077. https://doi.org/10.1144/jgs2021-077.
[69] Ketzer M, Praeg D, Augustin AH, Rodrigues LF, Steiger AK, Rahmati-Abkenar M, et al. Gravity complexes as a focus of seafloor fluid seepage: the Rio Grande Cone, SE Brazil. Sci Rep 2023;13:4590. https://doi.org/10.1038/s41598-023-31815-1.
[70] Stevens TO, McKinley JP. Abiotic controls on H $_2$ production from Basalt–Water reactions and implications for aquifer biogeochemistry. Environ Sci Technol 2000; 34:826–31. https://doi.org/10.1021/es990583g.
[71] Reed MH, Palandri J. Hydrogen produced by reduction of H2O in rock reaction: peridotite vs basalt. In: AIP conference proceedings, vol. 987. Sendai (Japan): AIP; 2008. p. 100–4. https://doi.org/10.1063/1.2896951.